

A nanosensor for determination of glucose based on silver nanoparticles as fluorescence probes

J. Tashkhourian¹ · M. Akhond¹ · S. Hooshmand¹ · M. Afsharinejad¹

Received: 23 December 2014 / Accepted: 3 June 2015 / Published online: 16 June 2015
© Iranian Chemical Society 2015

Abstract A nanosensor was designed for the enzymatic determination of glucose based on the fluorescence enhancement of silver nanoparticles (AgNPs). This enhancement is the result of the glucose oxidase-catalyzed oxidation of glucose. Silver nanoparticles were prepared through a chemical reduction by using trisodium citrate as the reducing agent and were characterized with UV–visible spectroscopy, Fourier transform infrared spectroscopy and transmission electron microscopy. The experimental results showed that the increase of the AgNP fluorescence was linearly proportional to the concentration of glucose within its concentration ranges of 2.50×10^{-5} – 7.50×10^{-3} M and 7.50×10^{-3} – 7.50×10^{-2} M with a detection limit of 5.53×10^{-7} M under the optimized experimental conditions. To evaluate the applicability of the nanobiosensor, determination of glucose in real samples was performed according to the developed procedure.

Keywords Silver nanoparticles · Glucose · Glucose oxidase · Fluorescence · Nanosensor

Introduction

Today's nanotechnology harnesses current progress in chemistry, physics, materials science, and biotechnology to create novel materials that have unique properties. Manipulation of materials and processes on a nanometer scale is opening a world of creative possibilities. The benefits

afforded by nanoscale technologies are expected to have substantial impacts on almost all industries and areas of society (e.g., medicine, plastics, energy, electronics, and aerospace) [1–5]. The recent advancement of bioanalytical techniques involving the development of highly sensitive or selective analytical methods based on nanoscale materials/molecules have progressed with remarkable success. In this regard, silver nanoparticles (AgNPs) have received significant attention in constructing analytical and bioanalytical sensors. This relevance arises from their unusual optical, electronic, and chemical properties [6–8]. They have a high surface area, very small size (<20 nm) and high dispersion ability, spectrally selective coating [9, 10], surface-enhanced Raman scattering [11, 12], and antibacterial activity [13]. Moreover, AgNPs exhibit optical properties which could not be observed either in molecular or in bulk metallic form [14–17].

Fluorescence spectroscopy as a sensitive, simple, diverse, and nondestructive method can provide real time, in situ, and dynamic analytical information [18]. However, utilizing nanoparticles in fluorescence analysis has provided significant improvement in this area [19–23]. It should be mentioned that the fluorescence of metal clusters and thin films is well established based on Mooradian's observation of photoluminescence from bulk copper and gold [24]. Also several reports are available related to the fluorescence of silver nanoclusters [25, 26].

Glucose, a simple sugar (monosaccharide), is an important carbohydrate in biology. Cells use it as a source of energy and a metabolic intermediate and its lack or excess can produce detrimental influence on cellular functions. The glucose level in blood is considered as a clinical indicator for diabetes. Therefore, the monitoring of glucose level in blood with faster and more accurate methods is in great demand and a great deal of effort has been focused

✉ J. Tashkhourian
tashkhourian@susc.ac.ir

¹ Department of Chemistry, College of Sciences, Shiraz University, Shiraz 71456, Iran

on improving smart methods for precisely monitoring the glucose level, with high sensitivity, high reliability, fast response, good selectivity, and low cost [27–32]. The most widely used methods for the determination of glucose are based on the monitoring of hydrogen peroxide stoichiometrically produced during the oxidation of glucose by oxygen in the presence of glucose oxidase. Many glucose-assay methods, such as surface plasmon resonance (SPR) spectroscopy [33, 34], fluorescence signal transmission [35–37], electrochemical signal transduction [38], near-infrared absorbance and Raman scattering [39, 40] have been also reported.

In this study a simple, sensitive, and selective sensor for fluorescence sensing of glucose is presented. The water-dispersible silver nanoparticles were used as a reliable agent for the enzymatic determination of glucose. The operational mechanism of the sensor is based on the enhancement fluorescence of silver nanoparticles that is caused by the glucose oxidase (GOx)-catalyzed oxidation of glucose. The sensor was applied for determination of glucose in artificial urine and human serum samples.

Experimental

Materials and reagents

All chemicals used were of analytical reagent grade and were used without further purification. Silver nitrate, trisodium citrate dihydrate, hydrogen peroxide, gluconic acid, glucose, sodium hydroxide, phosphoric acid, urea, ascorbic acid, fructose, lactose, saccharose, were all from Merck chemical companies. Glucose oxidase (GOx) was purchased from Sigma-Aldrich.

Preparation of silver nanoparticles

The silver colloid was prepared using a chemical reduction method described by Lee and Meisel [41]. Briefly, stock solutions of 1.0×10^{-3} M AgNO_3 and 1 % trisodium citrate dihydrate are prepared. An aliquot of 500.0 ml of AgNO_3 aqueous solution is heated up to 100 °C, and then 10.0 mL of trisodium citrate solution was added to it drop by drop with vigorous magnetic stirring at 800 rpm. Heating and stirring were continued for 30.0 min. Upon cooling of the solution, a green–gray colloidal solution of silver nanoparticles having a concentration of about 3.0 nM is produced [42].

Apparatus and fluorescence measurements

All fluorescence spectra were recorded on a Perkin-Elmer Spectrofluorimeter (model LS50B) equipped with a 1 cm

quartz cell. The emission spectra in the range of 300–550 nm were recorded under a fixed excitation wavelength of 280 nm. The slitwidths of both excitation and emission were 15 nm. The pH of the buffer solutions was measured by a Metrohm (780) pH meter. The absorbance spectra were recorded on a Pharmacia Ultraspec double beam spectrophotometer model 4000UV/Vis. Magnetic stirring was carried out using a Heidolph MR Hei-standard magnetic stirrer. A Philips (model CM 10) transmission electron microscopy (TEM) was used for measuring the size and dispersivity of the silver nanoparticles. A Perkin-Elmer (940 Spectrum RX1) was used for FTIR characterization of the suspension and the resulting nanoparticles. An Eppendorf micropipette was used for injecting the sample solutions.

Procedure

To study the enhancement effect of enzymatic reaction of glucose on AgNPs, 9.0 μL of the stock solution of silver nanoparticle was diluted to 10.0 mL with 1.0×10^{-1} M phosphate buffer (PB, pH 7.0), and then 133.0 μL of GOx solution (3.0 mg/mL, pH 7.0) was added into the diluted nanoparticles. Then glucose solutions with different concentrations were added into the nanoparticles/GOx mixture for fluorescent detection.

Results and discussion

In order to develop a sensitive and rapid spectrofluorimetric method for determination of glucose, the experimental conditions for fluorescence emission of AgNPs in the presence of glucose was improved by studying the effect of various factors such as pH, GOx concentration, reaction time, temperature and silver nanoparticles concentration.

Characterization and spectral features of silver nanoparticles

Nearly monodisperse silver nanoparticles were obtained via chemical reduction of silver salt solution. The structure and morphology of the resulting AgNPs were investigated through a transmission electron microscope (TEM) as shown in Fig. 1. The figure indicates that the particles are monodisperse and the majority of them have a size smaller than 30 nm. The Fourier transform infrared (FTIR) spectra were carried out to identify the capped silver nanoparticles, i.e., to provide information about the local molecular environment of the organic molecules on the surface of nanoparticles. The FTIR spectra of pure citrate and citrate-capped silver nanoparticles are shown in Fig. 2. According to this figure, the pure citrate sample shows

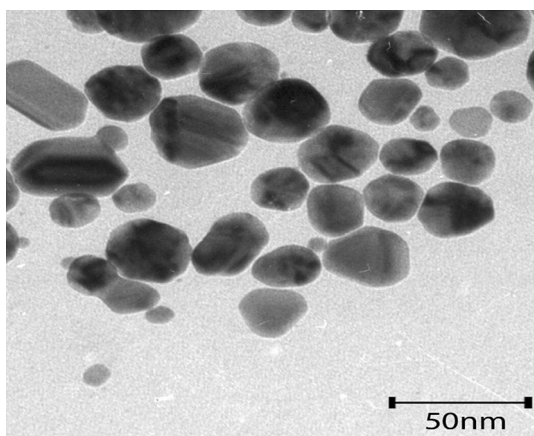


Fig. 1 TEM image of silver nanoparticles

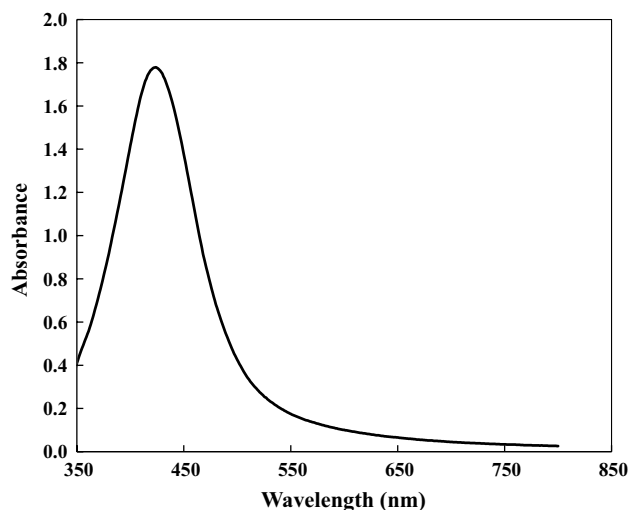


Fig. 3 The UV-Vis absorption spectrum of AgNPs

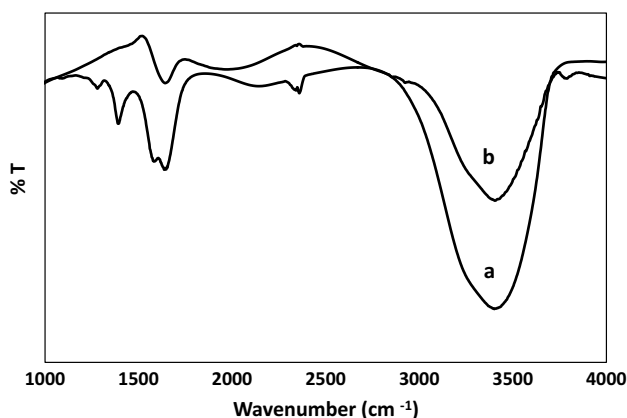


Fig. 2 FTIR spectra of a citrate, b citrate-capped AgNPs

strong absorption peaks at 3400, 1654, and 1292 cm^{-1} corresponding to hydroxyl bands, the symmetric stretching of carboxylate anion ($-\text{COO}^-$), C–O stretching, respectively. The spectrum of the capped AgNPs shows a shift due to the chemical adsorption of citrate with the surface of AgNPs which is an indication for preparation of citrate-capped silver nanoparticles. Figures 3 and 4 show a typical normalized absorption and luminescence spectra of the synthesized citrate-capped silver nanoparticles. The absorption spectrum shows that the silver nanoparticles have a wide range of absorption with a maximum absorption peak at 412 nm.

Origin of the analytical signal

It has been observed that the fluorescence intensity of the original silver nanoparticles was increased successively with increasing glucose concentration in the presence of GOx. The schematic of the reaction mechanism is given in Fig. 5.

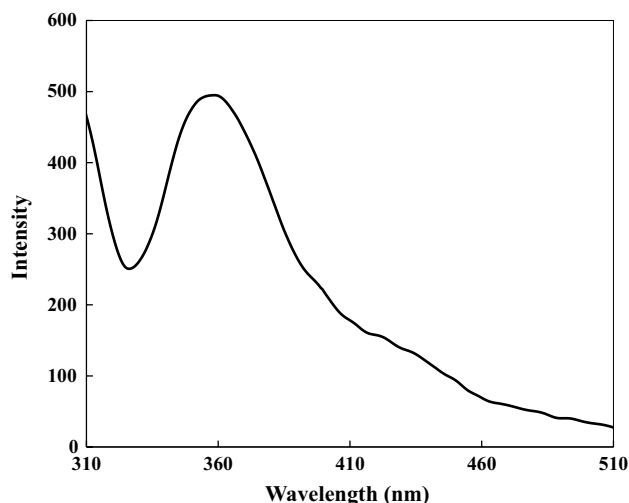


Fig. 4 The fluorescence spectrum of citrate-capped silver nanoparticles, $\lambda_{\text{ex}} = 280 \text{ nm}$, $\lambda_{\text{em}} = 360 \text{ nm}$

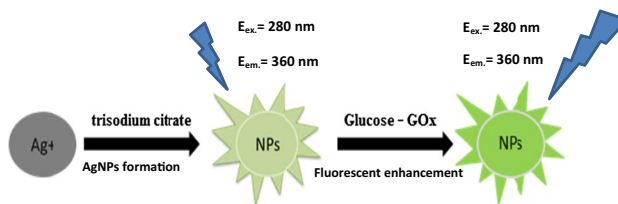


Fig. 5 Schematic of the constructed biosensor

The enzymatic reaction of glucose has two products: H_2O_2 and gluconic acid [43]. The most widely used methods for the determination of glucose are based on the monitoring of hydrogen peroxide stoichiometrically produced during the

oxidation of glucose by dissolved oxygen in the presence of glucose oxidase. There are some reports about enzymatic reaction of glucose in the presence of AgNPs based on surface plasmon resonance (SPR) change of this nanoparticle [27, 44–46]. Unfortunately, little work has been reported regarding investigation of the fluorescence properties of silver nanoparticles in enzymatic reactions. Experimental results for titration of AgNPs with various concentrations of H_2O_2 shows that H_2O_2 caused the fluorescence intensity of silver nanoparticles to increase. Moreover, the titration of silver nanoparticles with various concentrations of gluconic acid showed that the fluorescence intensity of AgNPs slightly increased. These investigations indicated that the enhancement of fluorescence of AgNPs in the enzymatic reaction was due to H_2O_2 production.

Effect of AgNP concentration

It was found that concentration of AgNPs affected not only the fluorescence intensity, but also the sensitivity of the method. When concentration of Ag nanoparticles is too high and pH is 7.0, the fluorescence intensity increases and the linear range significantly narrowed probably as a result of self-quenching of the AgNPs' fluorescence [47]. On the other hand, when the concentration of AgNPs is too low, the fluorescence intensity as well as sensitivity decreases (Fig. 6). Based on these results, 3.0 μ L of prepared silver nanoparticles solution in 3.0 mL solution was applied for further studies.

Effect of pH

Enzyme activity is always affected by several parameters such as the pH of the sample solution. The fluorescence

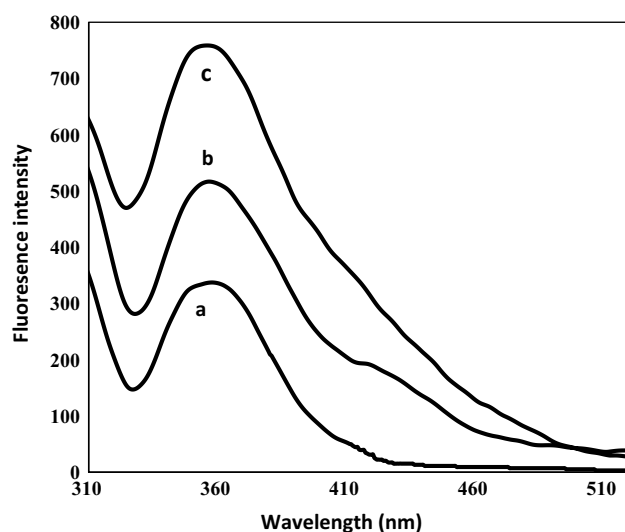


Fig. 6 The effect of AgNP concentration on the fluorescence intensity: **a** 1.5 μ L, **b** 3.0 μ L, **c** 5.0 μ L in cell containing 3.0 mL of solution. λ_{ex} = 280 nm, λ_{em} = 360 nm

intensity of silver nanoparticles is pH-dependent too. Therefore, the pH of the working assay must be adjusted to a suitable value. Here, 9.0 μ L of the prepared silver nanoparticles solution was added into 10.0 mL solution with various pH values of 3.0–9.0. The solution pH was varied in the range of 3.0–9.0 with phosphate buffer as shown in Fig. 7, where I_0 is the intensity of the fluorescence in the absence of glucose, and I is the intensity of the fluorescence when glucose is present at a constant concentration. The excitation wavelength of the measurements was set at 280 nm. As is shown in Fig. 7, the fluorescence intensity increased dramatically and reached a maximum value at pH 7.0. With further pH increase, the fluorescence intensity decreased sharply. So, pH 7.0 was selected for further studies. The low fluorescence intensities, in low acidic and high basic media are the results of enzyme activity of GOx. Since enzymes are proteins, they are sensitive to pH changes. Each enzyme has its own optimum pH range where it has its highest activity. This is the result of the effect of pH on a combination of factors: (1) the binding of the enzyme to the substrate, (2) the catalytic activity of the enzyme, (3) the ionization of the substrate, and (4) the variation of protein structure. The GOx enzyme is typically most active in the pH range of 4–7. Extremely high or low pH values result in complete loss of enzyme activity.

Effect of GOx concentration

In order to investigate the effect of glucose oxidase concentration, the effect of enzyme activity on the fluorescence intensity was examined. The result shown in Fig. 8 indicates that is obvious the rate increases until a certain point, and then levels off due to the saturation of the substrate with enzyme. Relatively constant fluorescence intensities

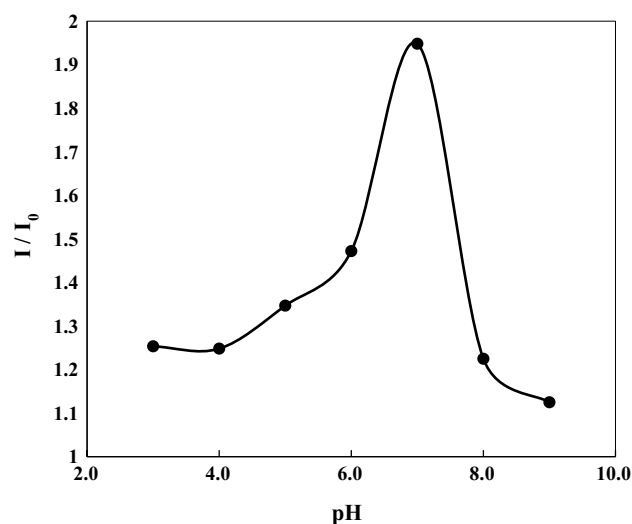


Fig. 7 Relationship between fluorescence intensity of AgNPs and the pH values. Experimental conditions: λ_{ex} = 280 nm, λ_{em} = 360 nm

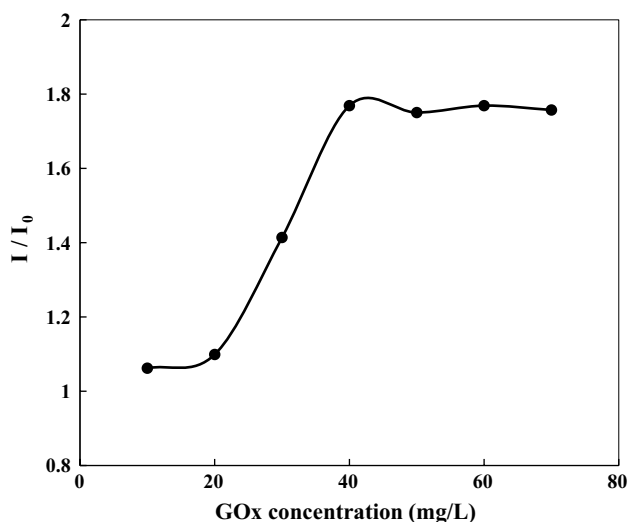


Fig. 8 Effects of glucose oxidase concentration on the fluorescence intensity of AgNPs–glucose system under standard assay conditions

were obtained for GOx activity values above 40 $\mu\text{g}/\text{mL}$. As the concentration (amount) of enzyme increases, more enzyme is available to accept substrate molecules. At low enzyme concentrations, the reaction rate is slow.

Effect of reaction time

The response time of the glucose biosensor was calculated by plotting the fluorescence intensity against reaction time at 1.0×10^{-3} M of glucose. As shown in Fig. 9, the saturated fluorescence enhancement reached 95 % of the steady-state signal in about 7 min.

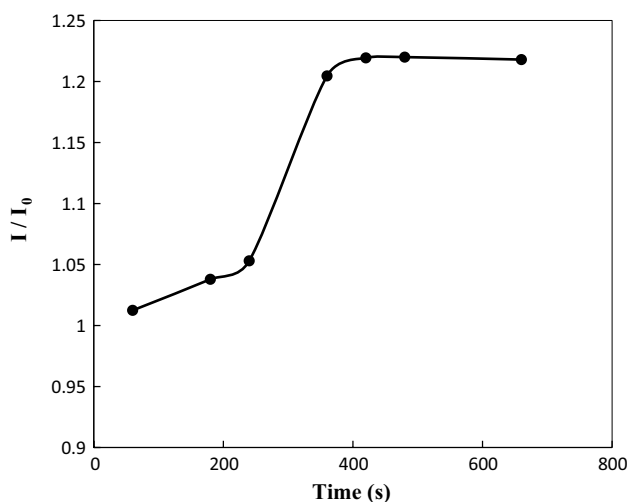


Fig. 9 The time-dependence response characteristics of the optical sensor. Condition: phosphate buffer solution (pH 7.0) containing 1.0×10^{-3} M glucose, at $\lambda_{\text{ex}} = 280$ nm, $\lambda_{\text{em}} = 360$ nm

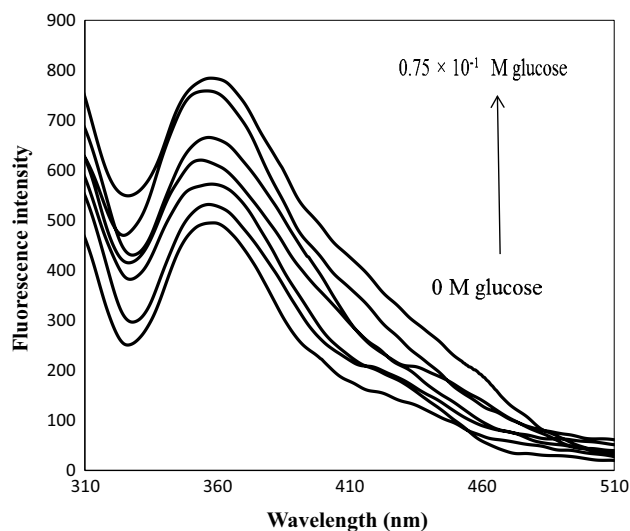


Fig. 10 Fluorescence enhancement of the silver nanoparticles upon stepwise addition of glucose/GOx. All smoothed spectra were recorded under the identical experimental conditions at $\lambda_{\text{ex}} = 280$ nm, $\lambda_{\text{em}} = 360$ nm

Calibration curve and detection limit

Under the optimal experimental conditions, the fluorescence spectra of AgNPs for different amounts of glucose were recorded. The results are shown in Figs. 10 and 11. The calibration curve for the quantification of glucose was linear in two ranges of concentration. Linear relationships in the concentration range of 2.50×10^{-5} – 7.50×10^{-3} M and 7.50×10^{-3} – 7.50×10^{-2} M with correlation coefficients of 0.990 and 0.997, respectively, were obtained. The limit of detection (LOD) is defined by the equation $\text{LOD} = (3/\sigma k)$, where σ the standard deviation of the blank measurements and k is the slope of the calibration graph. The LOD (for $n = 10$) was 5.53×10^{-7} M based on the linear concentration range of 7.50×10^{-3} – 2.50×10^{-5} M.

Repeatability

The average fluorescence intensity for six determinations of 1.0×10^{-3} M glucose under the optimum experimental conditions was 618.2 (a.u.) with a relative standard deviation of 1.2 % indicating that the method has a good repeatability as shown in Fig. 12.

Interference study

In order to investigate the practical application in determination of glucose, the possible interferences from species such as ascorbic acid, acetic acid, uric acid, saccharose, fructose, and lactose were tested. Results (Table 1) showed that these compounds had no significant interference up

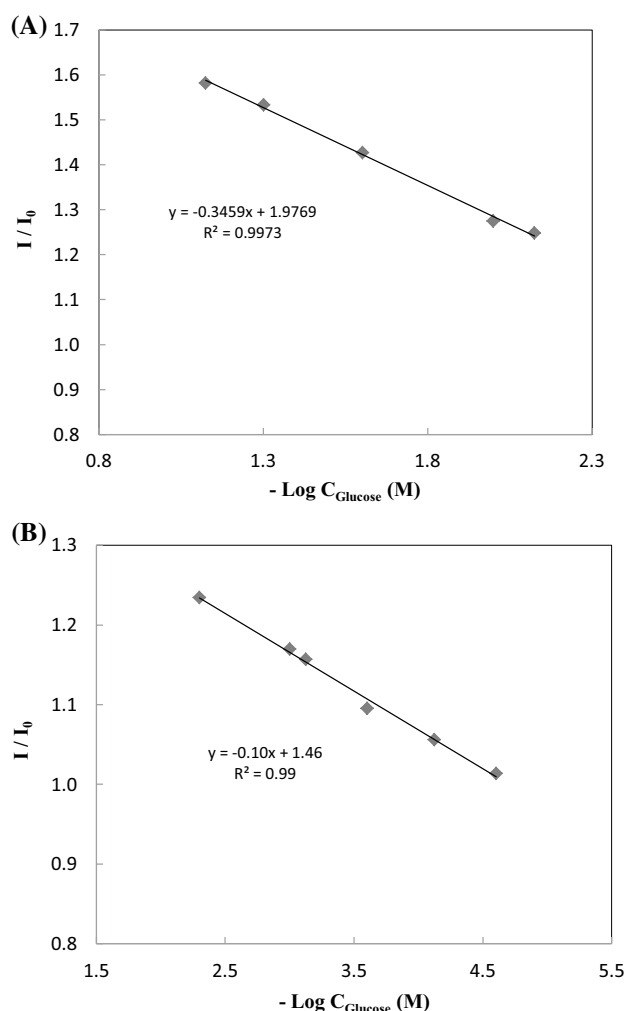


Fig. 11 Linear calibration curve for glucose, **a** concentration range from 7.50×10^{-3} to 7.50×10^{-2} M, **b** concentration range of 7.50×10^{-3} – 2.50×10^{-5} M, $\lambda_{\text{ex}} = 280$ nm, $\lambda_{\text{em}} = 360$ nm pH 7.0

to 100-fold glucose concentration indicating that the sensor selectivity responds to glucose in the presence of other commonly existing species.

Analysis of artificial urine

Artificial urine was synthesis based on a literature-reported approach [48]. The results for glucose determination in this sample are listed in Table 2. According to the results, the recovery of the spiked glucose in the urine sample was in the range of 97.3–104.2 %.

Analysis of serum sample

To evaluate the applicability of the assembled nanobiosensor, determination of glucose in serum samples was performed according to the developed procedure. Fresh human

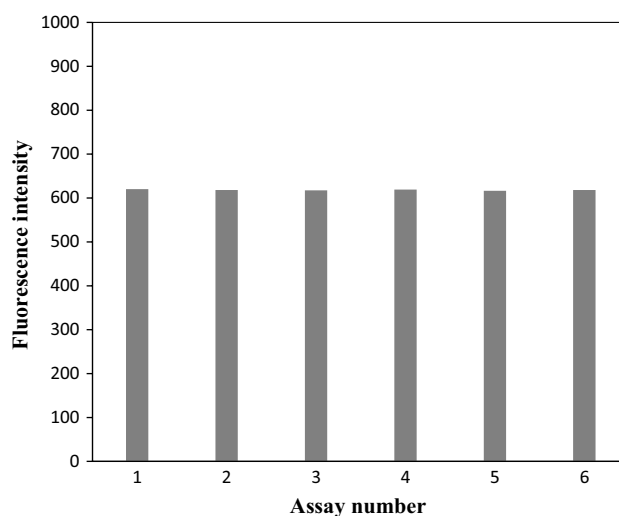


Fig. 12 Investigation of repeatability, condition: phosphate buffer solution (pH 7.0) containing 1.0×10^{-3} M glucose, at $\lambda_{\text{ex}} = 280$ nm, $\lambda_{\text{em}} = 360$ nm

serum samples were supplied by the local hospital. Since hemoglobin and other proteins in serum sample interfere with glucose determination, the serum samples were deproteinized before analysis [49]. The recovery results of this analysis are given in Table 3 which are in the range of 95.1–104.4 %.

Table 1 Tests for the interference of foreign ions (glucose: 1.0×10^{-3} M)

Species	Concentration ratio of coexisting substance to glucose	$\Delta I^a/I_0$
Acetic acid	100.0	0.0369
Ascorbic acid	100.0	0.0062
Uric acid	100.0	0.0143
Saccharose	100.0	0.0015
Fructose	100.0	0.0045

$\Delta I^a = I - I_0$ where I_0 and I are the fluorescence intensity of silver nanoparticles–GOx–glucose system in the absence and presence of interfering species

Table 2 Determination of glucose in artificial urine

Real sample	Spiked (M)	Found (M)	Recovery
1	–	ND	–
2	5.00×10^{-4}	5.11×10^{-4}	102.2
3	1.00×10^{-4}	9.70×10^{-5}	97.3
4	5.00×10^{-6}	5.20×10^{-6}	104.2

ND not detected

Table 3 Analytical results for determination of glucose in the human serum samples

Real sample	Measured (M) ^a	Spiked (M)	Found (M)	Recovery (%)
1	3.50×10^{-4}	0.00	3.60×10^{-4}	–
		3.00×10^{-3}	3.22×10^{-3}	95.1
		6.00×10^{-3}	6.43×10^{-3}	101.1
		9.00×10^{-3}	9.27×10^{-3}	98.9
2	1.25×10^{-3}	0.00	1.28×10^{-3}	–
		3.00×10^{-3}	4.37×10^{-3}	102.8
		6.00×10^{-3}	7.17×10^{-3}	98.1
		9.00×10^{-3}	10.67×10^{-3}	104.4

^a Measured value by the proposed method**Table 4** Comparison of different fluorescent methods for the determination of Glucose

System	Linear range	Detection limit	References
Hemin-functionalized graphene quantum dots	9.0–300.0 μ M	0.1 μ M	[50]
Enzyme-coupling reaction DT-diaphorase (DTD)	0.5–15.0 μ M	0.2 μ M	[51]
Quenching of gold nanoparticles	0.0–11.11 mM	–	[52]
pH induced on formational switch of i-motif DNA	5.0–100.0 μ M	4.0 μ M	[53]
Fe ₃ O ₄ peroxidase mimetic strategy	0.05–10.0 μ M	0.025 μ M	[54]
Nanometer-sized TiO ₂ and polyaniline	0.02–6.0 mM	18.0 μ M	[55]
Gold nanoclusters-based photoelectrochemical sensors	75.0–408.0 μ M	–	[56]
CdS quantum dots-based glucose sensing	0.1 μ M–1.0 mM	20.0 nM	[57]
Anionic dye and a cationic quencher/receptor	1.0–20.0 mM	1.0 mM	[58]
Porphyrin-modified NiO nanoparticles	0.05–5.0 mM	0.02 mM	[59]
3-Aminophenylboronic acid-functionalized CuInS ₂ QDs	0.005–8.0 mM	1.2 μ M	[60]
Polyethyleneimine-templated Cu nanoclusters	10.0–100.0 μ M	8.0 μ M	[61]
This method	25.0 μ M–75.0 mM	0.5 μ M	–

Conclusion

It was attempted to establish a novel method for quantitative analysis of glucose based on the fluorescence enhancement of silver nanoparticles. The method has many advantages, including high sensitivity and selectivity, simple operation, and low cost. Silver nanoparticles were stable over 3 weeks and could be used for determination of glucose over a wide concentration range. Comparison of different fluorescent methods for the determination of glucose with the proposed method is presented in Table 4. The relatively low detection limit, wide detection range and the facile and rapid determination procedure make this detection system promising for direct, practical glucose determination in biological samples.

Acknowledgments We would like to acknowledge Prof. G. Absalan for his outstanding editing and guidance. Also we gratefully acknowledge the support of this work by Shiraz University Research Council.

References

- D.N.T. Kumar, Q. Wei, Res. J. Biotechnol. **8**, 78 (2013)
- L. Bau, P. Tecilla, F. Mancin, Nanoscale **3**, 121 (2011)
- T. Khosousi, PhD Thesis, Shiraz University, Shiraz (2012)
- N. Lkhagvajav, I. Yasa, E. Çelik, M. Koizhaiganova, Ö. Sari, Dig. J. Nanomater. Bios. **6**, 149 (2011)
- Y.Q. Wang, C. Ye, Z.H. Zhu, Y.Z. Hu, Anal. Chim. Acta **610**, 50 (2008)
- T. Taton, C. Mirkin, R. Letsinger, Science **289**, 1757 (2000)
- S. Schultz, D. Smith, J. Mock, D. Schultz, Proc. Natl. Acad. Sci. USA. **97**, 996 (2000)
- J. Yguerabide, E.E. Yguerabide, Anal. Biochem. **262**, 157 (1998)
- J.R. Cole, N.J. Halas, Appl. Phys. Lett. **89**, 153120 (2006)
- B.P. Rand, P. Peumans, S.R. Forrest, J. Appl. Phys. **96**, 7519 (2004)
- S. Yamamoto, H. Watarai, Langmuir **22**, 6562 (2006)
- M.W. Meyer, E.A. Smith, Analyst **136**, 3542 (2011)
- M.S. Abdel-Aziz, M.S. Shaheen, A.A. El-Nekeety, M.A. Abdel-Wahhab, J. Saudi Chem. Soc. **18**, 356 (2014)
- J.P. Wilcoxon, B.L. Abrams, Chem. Soc. Rev. **35**, 1162 (2006)
- J. Zheng, P.R. Nicovich, R.M. Dickson, Annu. Rev. Phys. Chem. **58**, 409 (2007)
- S. Fedrigo, W. Harbich, J.J. Buttet, J. Chem. Phys. **99**, 5712 (1993)

17. J. Zheng, Y. Ding, B. Tian, L.W. Zhong, X. Zhuang, *J. Am. Chem. Soc.* **130**, 10472 (2008)
18. M. Lowry, S.O. Fakayode, M.L. Geng, G.A. Baker, L. Wang, M.E. McCarrroll, G. Patonay, I.M. Warner, *Anal. Chem.* **80**, 4551 (2008)
19. J. Yan, M.C. Estevez, J.E. Smith, K. Wang, X. He, L. Wang, W. Tan, *Nano Today* **2**, 44 (2007)
20. L. Shang, Sh Dong, G. Ulrich, Nienhaus. *Nano Today* **6**, 401 (2011)
21. X. Yan, H. Li, Y. Li, X. Su, *Anal. Chim. Acta* **852**, 189 (2014)
22. B. Liu, H. Tan, Y. Chen, *Anal. Chim. Acta* **761**, 178 (2013)
23. L. Zhang, E. Wang, *Nano Today* **9**, 132 (2014)
24. A. Mooradian, *Phys. Rev. Lett.* **22**, 185 (1968)
25. OP Siwach, P. Sen, *J. of Lumin.* **129**, 6 (2009)
26. Z. Jiang, W. Yuan, H. Pan, *Spectrochim. Acta A* **61**, 2488 (2005)
27. J. Tashkhourian, M.R. Hormozi Nezhad, J. Khodaveisi, R. Dashti, *Sen. Actuat. B* **158**, 185 (2011)
28. M. Ben-Moshe, V.L. Alexeev, S.A. Asher, *Anal. Chem.* **78**, 5149 (2006)
29. E.A. Moschou, B.V. Sharma, S.K. Deo, S. Daunert, *J. Fluoresc.* **14**, 535 (2004)
30. T. Zhang, E.V. Anslyn, *Org. Lett.* **9**, 1627 (2007)
31. M. Hu, J. Tian, H.T. Lu, L.X. Weng, L.H. Wang, *Talanta* **82**, 997 (2010)
32. J. Tashkhourian, M. Akhond, S. Hooshmand, T. Khosousi, B. Hemmateenejad, *Anal. Bioanal. Chem. Res.* **1**, 117 (2014)
33. S. Lee, V.H. Perez-Luna, *Anal. Chem.* **77**, 7204 (2005)
34. K. Asian, J.R. Lakowicz, C.D. Geddes, *Anal. Chem.* **77**, 2007 (2005)
35. G. Blagoi, N. Rosenzweig, Z. Rosenzweig, *Anal. Chem.* **77**, 393 (2005)
36. P.W. Barone, R.S. Parker, M.S. Strano, *Anal. Chem.* **77**, 7556 (2005)
37. B.L. Ibey, H.T. Beier, R.M. Rounds, G.L. Cote, V.K. Yadavalli, M.V. Pishko, *Anal. Chem.* **77**, 7039 (2005)
38. W. Chen, H. Yao, C.H. Tzang, J. Zhu, M. Yang, S.-T. Lee, *Appl. Phys. Lett.* **88**, 213104 (2006)
39. I. Amato, *Science* **258**, 892 (1992)
40. M.R. Robinson, R.P. Eaton, D.M. Haaland, G.W. Koepp, E.V. Thomas, B.R. Staliard, P.L. Robinson, *Clin. Chem.* **38**, 1618 (1992)
41. P.C. Lee, D. Meisel, *J. Phys. Chem.* **86**, 3391 (1982)
42. D. Paramelle, A. Sadovoy, S. Gorelik, P. Free, J. Hogley, D.G. Fernig, *Analyst* **139**, 4855 (2014)
43. Z. Tao, R. A. Raffel, A.-K Souid, J. Goodisman, *Biophys J.* **8**, 2977 (2009)
44. Y. Zhang, Y.-J. Zhang, X.-D. Xia, X.-Q Hou, C.-T. Feng, J.-X. Wang, L. Deng, *Chin. Chem. Lett.* **24**, 1053 (2013)
45. S. Ma, J. Mu, Y. Qu, L. Jiang, *Colloids Surf. A* **345**, 101 (2009)
46. Y. Xia, J. Ye, K. Tan, J. Wang, G. Yang, *Anal. Chem.* **2**, 6241 (2013)
47. O. Parkash Siwach, P. Sen, *Spectrochim. Acta Part A* **69**, 659 (2008)
48. S. Chutipongtanate, V. Thongboonkerd, *Anal. Biochem.* **402**, 110 (2010)
49. M.V. Martinez-Ortega, M.C. Garcia-Parrilla, A.M. Troncoso, *Anal. Chim. Acta* **502**, 49 (2004)
50. Y. He, X. Wang, J. Sun, Sh Jiao, H. Chen, F. Gao, L. Wang, *Anal. Chim. Acta* **810**, 71 (2014)
51. X. Gao, X. Li, Q. Wan, Z. Li, H. Man, *Talanta* **120**, 456 (2014)
52. Z. Bagheri, R. Massudi, J. Ghanavi, *Optics & Laser Tech.* **58**, 135 (2014)
53. Q. Keb, Y. Zheng, F. Yang, H. Zhang, X. Yang, *Talanta* **129**, 539 (2014)
54. Y. Shi, P. Su, Y. Wang, Y. Yang, *Talanta* **130**, 259 (2014)
55. W. Tang, L. Li, X. Zeng, *Talanta* **131**, 417 (2015)
56. J. Zhang, L. Tu, Sh Zhao, G. Liu, Y. Wang, Y. Wang, Z. Yue, *Biosens. Bioelectron.* **67**, 296 (2015)
57. G.-L. Wang, X.-L. Hu, X.-M. Wu, Z.-J. Li, *Sens. Actuat. B* **205**, 61 (2014)
58. X. Wang, L. Feng, L. Zhang, *Sens. Actuat. B* **208**, 588 (2015)
59. Q. Liu, Y. Yang, H. Li, R. Zhu, Q. Shao, Sh Yang, J. Xu, *Biosens. Bioelectron.* **64**, 147 (2015)
60. Z. Liu, L. Liu, M. Sun, X. Su, *Biosens. Bioelectron.* **65**, 145 (2015)
61. Y. Ling, N. Zhang, F. Qu, T. Wen, Z. Feng Gao, N. Bing Li, H. Qun Luo, *Spectrochim. Acta A* **118**, 315 (2014)